INVESTIGATING LOCAL ASYMMETRIC SURFACE ROUGHNESS ON COMET 67P/C-G USING 3D MONTE CARLO SIMULATIONS OF DUST DYNAMICS. J. L. Kloos[1], T. L. Farnham[1], J. M. Sunshine, and J. Rizos[1], [1]Department of Astronomy, University of Maryland, College Park, Maryland (jlkloos@umd.edu)

Introduction: The transport and redistribution of dust around cometary nuclei is of great interest for understanding the uppermost layer of the surface, its thermal and physical properties, and its orgins. The fallback of dust also governs the appearance of the surface at both global and local scales; in fact, previous research has linked transport mechanisms with specific surface morphology on comet 67P/Churyumov-Gerasimenko (CG), namely wind tails and ripple structures [1].

There are other surface morphologic features on CG, however, that may also be explained by dust infall. Figure 1 displays OSIRIS imagery of three circular features that show asymmetric texture: part of the surface appears to be smooth and relatively free of debris, while the remaining region appears rough in comparison. One possible explanation for this asymmetry in roughness is the topographic shielding of dust infall, which keep sections of the depression relatively free of incoming dust particles. In this work, we apply a thermophysical model, in conjunction with a transport model, to explore the transport of dust around the nucleus, and investigate the role that topography plays in dust redistribution.

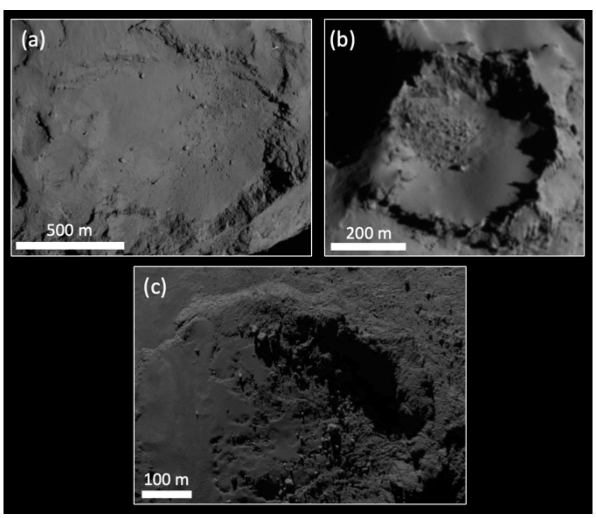

Figure 1: OSIRIS imagery of circular features on CG showing asymmetric interior roughness.

Thermal Model: Surface and sub-surface temperatures on the nucleus are computed using a 1-D thermal model that accounts for the physical and compositional properties of the surface. A 2-layer model is implemented that assumes a desiccated surface layer 5 mm thick that overlies a uniform mixture of ice and dust. To explore the thermal distribution across the surface, a digital shape model (DSM) is used with resolutions of 6,000 facets [2]. The incoming solar insolation at each facet is simulated as a function of time, while shadowing and self-heating are incorporated using a ray-tracing algorithm. Heat transfer into the subsurface occurs through solid conductivity of contacting dust/ice grains, as well as through radiative conductivity through pore spaces between grains [3]. To estimate the surface and subsurface temperatures, the 1-D heat equation is solved using a Crank-Nicolson scheme.

Transport Model: To examine the redistribution of non-volatile material around the comet nucleus, a mass transport model was developed based on existing models (e.g. [4]). Dust material (referred to here as "particles") is sourced from each facet of the shape model, where the number of particles emitted from each face is determined by the integrated sublimation mass flux across one orbital period. In total, 1.75 million particles were used in the simulation, representing 4.28e9 kg of non-escaping dust material. Therefore, a single particle is equivalent to ~2.45e3 kg of dust.

Coma densities are assumed to be small enough to ignore the influence of gas drag, and therefore particle trajectories evolve under the influence of gravitational, centrifugal and Coriolis forces. The acceleration due to gravity is computed using a Mascon gravity model assuming uniform interior mass density. The launch speed of each particle is randomized between v = 0.1 m/s and 0.7 m/s; the direction of emission is also randomized across 2π steradians, centered on the local surface normal. Figure 2 shows simulated flight paths of particles emitted from different locations of the nucleus at non-escaping speeds.

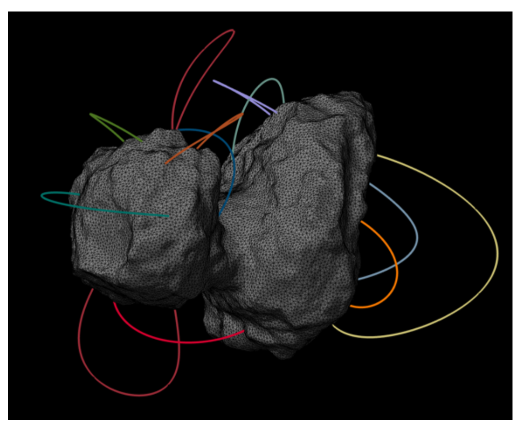

Figure 2: Modelled trajectories of non-escaping dust particles around the nucleus of comet 67P/C-G.

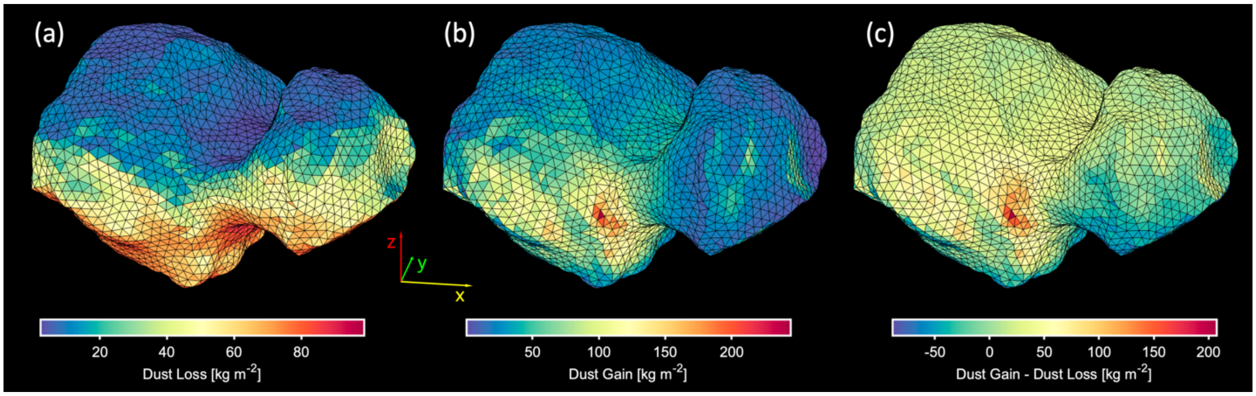

Figure 3: (a) Mass concentration of non-volatile material lost across one orbital cycle. This quantity represents the dust mass flux emitted from each face, integrated across one year. (b) Mass concentration of non-volatile material accumulated across one orbital cycle. (c) Net accumulation of non-volatile material across one orbital cycle.

To reflect the ongoing sublimation that occurs, particles impacting the surface may be re-emitted. The probability of re-emission is determined by scaling the integrated mass flux of each facet such that the values range between 0.1 and 0.9. This scheme ensures that regions with enhanced sublimation are less likely to collect material, while still maintaining the random nature of this process.

Results: Figure 3b shows the resulting concentration (kg per unit area) of dust material gained at each facet of the DSM. This quantity reflects the mass concentration that is accumulated at each facet across one orbit. As can be observed, the distribution is highly non-uniform: areas of enhanced deposition occur at the leading edge of each lobe, which include sections of Imhotep, Seth, Hapi and Bastet. These areas preferentially accumulate material due to the rotation of the nucleus, which sweeps up low-lying and slow-moving dust within the coma.

The net accumulation of non-volatile material can be found by balancing the mass concentration that is lost (Figure 3a) with that which is gained (Figure 3b); this is shown in Figure 3c. As can be observed here (and demonstrated elsewhere (e.g. [5]), the northern hemisphere accumulates more dust than is lost through entrainment. Most of the dust collecting on the northern hemispheric regions originates from the active southern regions. Based on these simulations, we estimate that approximately 4.8e9 kg of dust material is transferred from the southern hemisphere to the northern hemisphere per orbital year. Assuming a bulk density of 532 kg m^3 [6] this represents a dust layer up to ~30 cm thick that coats the northern hemisphere per year.

Asymmetry in dust infall is observed at local scales as well. Figure 4b provides a zoomed in region of a circular depression (noted earlier in Figure 1a) located on the small lobe. As shown here, the local dust accumulation is longitudinally asymmetric as a result of topographic shielding from the leading edge of the depression, with more than an order of magnitude variation between the eastern and western regions.

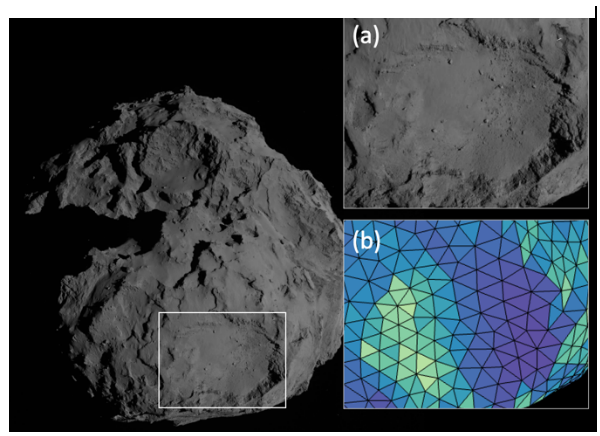

Figure 4: (a) OSIRIS image of a circular depression on the small lobe of CG showing asymmetric interior roughness. (b) Modelled dust accumulation (kg m^{-2}) for the same region showing asymmetric deposition due to topographic shielding.

Incorporating the influence of gas drag: The dust transport model discussed above has been updated to include the effects of gas drag on the motion of dust particles in the inner coma. Using this updated model, new simulations will be executed that will explore the redistribution of non-volatile material as a function of particle size and heliocentric distance. Using a high-resolution shape model, we will further investigate the role of local topography and nucleus rotation on the distribution of fallback of non-escaping dust, as well as how each of these varies as a function of dust-size distribution.

References: [1] Thomas, N., et al. (2015) *AA* 583. [2] Jorda, L. et al., (2015). NASA PDS and ESA PSA. [3] Hu, X. et al. (2019). *AA*, 630, A5. [4] Marschall, R. et al. (2020) *Frontiers in physics*, 8, 227. [5] Keller, H. U. (2017). *MNRAS*, 469(Suppl_2), S357-S371. [6] Jorda, L. et al., (2016). *Icarus*, 277, 257-278.